SEISMIC BEHAVIOR OF ANCHOR GROUPS – EXPERIMENTAL AND NUMERICAL STUDY

E.J. Stehle[(1)], A. Sharma[(2)]

[(1)] *Research Associate and PhD student, Institute of Construction Materials, University of Stuttgart, erik.stehle@iwb.uni-stuttgart.de*
[(2)] *Junior Professor, Institute of Construction Materials, University of Stuttgart, akanshu.sharma@iwb.uni-stuttgart.de*

Abstract

Post-installed anchors are often used to form a connection between the non-structural or structural component with the primary reinforced concrete (RC) structure. Especially when it comes to structural connections, one major field of application of the anchorages is in seismic retrofitting. In order to overcome the structural deficiencies and to ensure a ductile behavior of the structure, different retrofitting techniques have been developed. In general, irrespective of the strengthening solution employed, a certain type of post-installed anchorage is essential to connect the strengthening element with the primary structure. Additional steel bracing, haunch retrofit solution, dampers etc. are a few such examples where the seismic performance of the strengthening (or retrofitting) solution depends significantly on the seismic performance of the anchorage connecting the strengthening element and the structure. Similarly, in case of additional shear walls or additional structural elements (beams or columns), the seismic performance of the strengthened structure depends strongly on the seismic performance of the post-installed reinforcing bars used to form the connection between the old and new structural concrete.

In particular, the multiple-anchor groups used to directly connect the bracings, haunch elements or dampers are faced with certain challenges. The seismic demands of the structure lead to high cyclic tension and shear forces in the anchor group. The anchors often lie close to the plastic hinge region thus cracks of relatively large widths might intercept and influence the anchor performance. Limited dimensions of beams and columns prevent the exploitation of a full concrete cone breakout body and limit the transfer of bond forces by placing the anchor group close to the edges. Due to these high demands on the anchor group, standard force-based design approaches often are insufficient to obtain a practical and reliable solution for design of the connection, since the anchors used in structural strengthening solution would invariably be pushed beyond their linear range of performance. Furthermore, the performance of certain strengthening solutions might be significantly influenced by the displacement behavior of anchors. To correctly and reliably assess the suitability of the anchors for seismic strengthening applications, a displacement-based approach is necessary where the cyclic anchor behavior can be known throughout the complete range of the load-displacement curve and which accounts for a distribution of forces among the anchor group.

In this paper the load-displacement behavior of statically and cyclically loaded anchor groups in tension is studied experimentally and numerically. In the experiments, bonded anchors were used to form the connection and three different configurations were investigated in terms of their load-displacement and hysteretic behavior. A displacement-controlled loading protocol was utilized to determine the cyclic characteristics over the complete range of the load-displacement curve. It is found that the overall load-displacement behavior of cyclically loaded anchor groups resembles the load-displacement behavior of statically loaded anchor groups. However, upon unloading of the anchor groups, residual displacements at zero load were observed and when reloaded the anchor groups were not able to take up the same load as in the previous cycles. Furthermore, the experimental results form the basis of the numerical parameter study and are used to validate the numerical models. In the numerical parametric study, the influence of close edges and eccentric loading on the load-displacement characteristics of a 2 x 2 anchor group is investigated. The numerical analysis uses a microplane model with relaxed kinematic constraint as the constitutive law for concrete.

Keywords: anchor group; experimental investigation; numerical investigation; cyclic loading; displacement-controlled

1. Introduction

Post-installed anchors are a popular way to fasten both non-structural and structural elements to reinforced concrete (RC) structures. In non-structural applications, post-installed anchors are in general used to fasten components, such as pipes, facades, equipment or machinery to the primary structure. When it comes to earthquakes, the connected elements will start oscillating, placing high demands on the connection. In such a case the connection and the anchors may undergo large displacements. In structural applications, such as the strengthening of already existing buildings, a certain type of anchorage is essential to form the connection between the existing primary structure and the new strengthening element. A broad range of strengthening solutions has been developed, after severe earthquakes in the past decades have shown the vulnerability of RC structures to seismic actions [1, 2, 3]. This is especially true for RC frame structures, designed before the introduction of modern seismic codes, which are particularly prone to dynamic actions due to their non-seismical detailing [4, 5]. Additional shear walls or additional structural elements, such as beams or columns are examples, where post-installed reinforcing bars are a popular way to form the connection. In case of additional steel bracings [6], dampers or the haunch retrofit solution [7], post-installed anchors can be used to directly connect the new elements to the primary RC structure. In general, multiple-anchor groups are used to form the connection, irrespective of whether post-installed anchors are used in non-structural or structural applications, with groups of four or six anchors being the most common configurations.

When post-installed anchors are used to form the connection in structural strengthening applications, experiments have shown that the seismic performance of the strengthened structure highly depends on the seismic performance of the multiple-anchor group. In [6] a full-scale RC frame structure was retrofitted using steel bracing, which was directly attached to the primary structure by means of bonded expansion anchors. The performance of the strengthened structure was compared to the performance of the bare frame and a significant increase in the global strength and energy dissipation was observed, highlighting the feasibility of the strengthening solution with a direct connection using post-installed anchors. However, the experiment also showed the importance of the seismic performance of the connection for the success of the strengthening solution. At higher drift levels of the RC frame, the gusset plate misaligned due to the unrecoverable anchor displacement and caused buckling of the connection part of the steel bracing. Similar to the experiment using steel bracing to retrofit a RC frame, in [7] beam-column joint sub-assemblies were retrofitted using haunch elements, directly connected to the primary structure using post-installed anchors (fully fastened haunch retrofit solution). The experiments clearly showed the influence of the performance of the post-installed anchors on the overall behavior of strengthened sub-assemblies [8]. To attach the haunch element to the RC structure, three different types of post-installed anchors were used, while the dimensions and properties for the concrete specimen and the haunch element were kept the same. All three types of anchors were qualified for the use in seismic applications and the connections were designed for the same failure mode and approximately the same failure load. However, the performance of the retrofitted structure varied significantly depending on which type of anchor was used. This clearly shows that the seismic performance of the anchors has a major influence on the success of the retrofit solution and that the displacement and hysteretic behavior of an anchor must be taken into account in the design process. Therefore, a displacement-based qualification and design approach is necessary for anchorages used in seismic strengthening applications so that the anchor characteristics are known throughout the complete range of the load-displacement curve and which accounts for a distribution of forces among the anchor group.

Furthermore, the need for a displacement-based approach is motivated by the challenges faced by multiple-anchor groups used to, for example, directly connect steel bracings, haunch elements or dampers. Due to the nature of their application, the anchor groups are placed close to plastic hinge zones. This can lead to large cracks intercepting the anchors and hence influencing their performance. High tension and shear loads act on the anchor groups due to the high seismic demands of the structure. Limited dimensions of the RC members, in which the anchors are installed in, lead to anchor groups which are placed close to the edge. This has a negative influence on their load-bearing capacity by preventing a full concrete cone breakout body and limiting the transfer of bond forces. In addition, the anchor groups can be loaded eccentrically, resulting in an uneven distribution of forces among the anchors.

In this paper, the load-displacement behavior of multiple-anchor groups under static and cyclic tension load is investigated experimentally and numerically, with a focus on their potential use in structural or seismic strengthening applications. In the experimental program, the behavior of anchor groups with up to four anchors is investigated, when the groups are loaded centrically in tension. The influence of cyclic loading and different spacing on the load-displacement behavior is assessed. Hereby, a displacement-controlled loading protocol for pulsating tension load is applied, where the full range of the load-displacement curve can be covered. Note, that the applied cyclic loading protocol only covers design cases where the anchors take up the tension loads and the compression force is directly transferred by the baseplate to the concrete elements. It is not intended for design cases where the anchors have to transfer compression forces to the concrete as well. This is typically the case when post-installed anchors are used to connect haunch elements or steel bracings. Furthermore, the experimental results are utilized to validate the numerical models. In the numerical study, the influence of close edges and eccentric loading on the load-displacement characteristics and the distribution of forces is investigated on the quadruple anchor group which was first used in the experimental study.

2. Experiments

2.1 Experimental program

The focus of the experimental program is on the investigation of the multiple-anchor group load-displacement behavior under static and cyclic tension load. Hereby, the main interest lay in the concrete cone failure mode. On this basis, the test parameters, such as steel strength, concrete strength, anchor diameter and embedment depth were selected to obtain the desired failure mode. In order to investigate the load-displacement behavior of anchor groups, three different configurations were tested, comprising two anchors in a row with two different spacing and a quadruple anchor group. In total, six test series were performed with three test series under monotonic tension load and three test series under cyclic tension load. To obtain reference load-displacement curves, two additional test series on single anchors under static and cyclic load were carried out and hence a total of 24 tests have been performed. In Table 1, the experimental program and the test parameters are summarized.

2.2 Description of the test specimen and tested anchors

Unreinforced concrete slabs with a side length of 1635 mm and a height of 300 mm were used as the base material for the post-installed anchors. The specimens were made of normal strength concrete (C20/25). The strength of the concrete at the time of testing was determined using concrete cubes with a side length of 150 mm. The mean concrete cube compressive strength is given in Table 1. To ensure the comparability of the test results, all specimens were made from the same concrete batch. A bonded anchor system from manufacturer fischer was used, comprising the two-component injection system FIS EM Plus and a high-strength threaded rod (strength class 8.8). The injection system FIS EM Plus is qualified for the seismic category C1 and C2. Details on the technical design are provided in the corresponding technical assessment [9]. All anchors were installed according to the manufacture’s installation instructions. The baseplates for the anchor groups were made of S235JR steel. The dimensions for the various configurations are given in Table 1. To exclude any influence of close edges or neighboring anchor groups, the groups were positioned in a way, that the clear distance of the outermost anchors to the edge and the outermost anchors of the neighboring groups was at least 4 h_{ef}.

Table 1 – Experimental program and test parameters

Anchor system	Test No.	Configuration	Mean concrete cube compressive strength, $f_{cc,150,m}$ (kN/mm^2)	Anchor spacing s_1 (mm)	Anchor spacing s_2 (mm)	Type of load	Baseplate dimensions (mm)	Number of tests
Bonded anchor – M16 h_{ef} = 80 mm	BA-1x1-stat		26.81	-	-	Static	-	3
	BA-1x1-cyc			-	-	Cyclic	-	3
	BA-2x1-A-stat			80	-	Static	160 x 80 x 25	3
	BA-2x1-A-cyc			80	-	Cyclic	160 x 80 x 25	3
	BA-2x1-B-stat			160	-	Static	240 x 80 x 25	3
	BA-2x1-B-cyc			160	-	Cyclic	240 x 80 x 25	3
	BA-2x2-A-stat	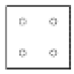		80	80	Static	160 x 160 x 25	3
	BA-2x2-A-cyc			80	80	Cyclic	160 x 160 x 25	3

2.3 Experimental setup and testing procedure

In order to obtain the desired concrete cone failure mode, an unconfined test setup was used. The experimental setup is shown in Fig.1 and comprises a test rig, a 250 kN servo-hydraulic cylinder to apply the load on the baseplate, a calibrated load cell with a measuring range up to 250 kN and displacement transducers (LVDT) to measure the anchor displacement and the displacement of the baseplate at the point of loading. The displacement of the baseplate was indirectly measured via a steel wire connecting the LVDT with the surface of the baseplate. The displacement was measured as close to the point of loading as possible. In case of the 2 x 1 configurations the displacement of all anchors was directly measured on top of the anchor, using two LVDTs as seen in Fig.1(b). A bridge-like stand was used to fix the LVDT to the concrete specimen. In case of the 2 x 2 configuration, the displacement of two anchors was directly measured as in case of the 2 x 1 configurations and the displacement of the remaining two anchors was indirectly measured via steel wires, connecting the LVDT with the top of the anchor. To apply the load, the servo-hydraulic cylinder and the baseplate were connected using a M20 threaded rod and a special hinge as seen in Fig.1(c).

In the static tests, a quasi-static loading rate of 2 mm/s was applied to pull the single anchors and the anchor groups out of the concrete. Two displacement values are derived from the static tests, s_u and s_{max}, which are required to define the displacement levels in the loading protocol for the cyclic tests. The value s_u is defined as the mean displacement corresponding to the mean ultimate load and the value s_{max} is defined as the higher value of either the mean displacement corresponding to a strength decay of 20% after reaching the ultimate load, $s_{80\%Nu}$, or two times the displacement value corresponding to the mean ultimate load, 2 s_u.

In Fig.2 the schematic structure of the cyclic loading protocol is presented. The cyclic loading protocol was first introduced in [10, 11], where it was utilized to test single anchors and to assess the seismic anchor behavior in the post-peak range of the load-displacement curve. Note, that the complete procedure is in displacement control. The protocol consists of nine stepwise increasing displacement levels and a residual pull-out test. In each displacement level, three cycles are performed. The first six displacement levels are defined by the value s_u and correspond to 10%, 20%, 30%, 50%, 70% and 100% of s_u. In the last three displacement levels, the displacement is further increased until s_{max} is reached. The last three displacement levels are equally spaced between s_u and s_{max}. The formulas to derive the displacement values are given in Fig.2. After the completion of the cyclic history, a pull-out test is performed to obtain the complete load-displacement curve and to bring the anchorage to failure.

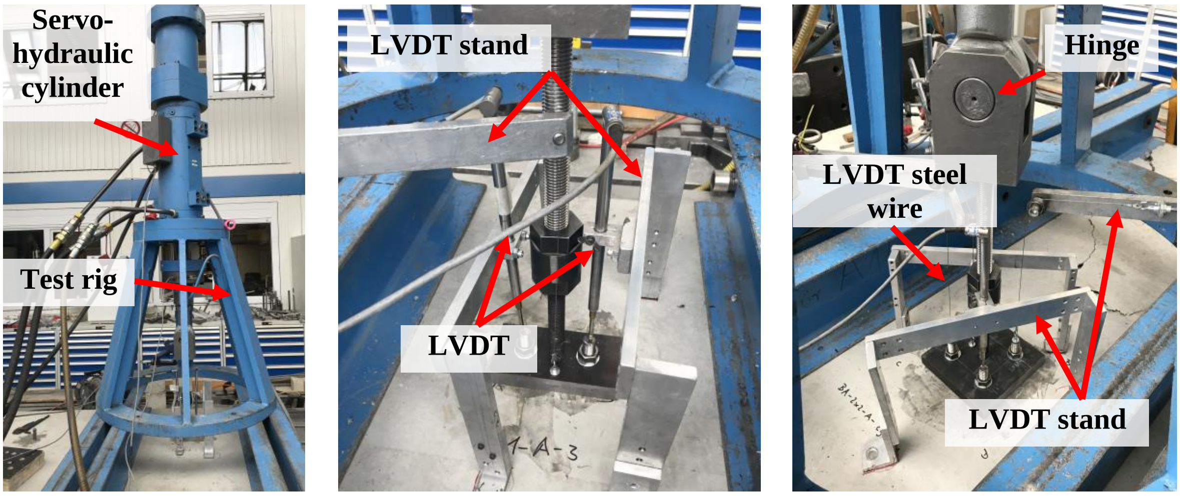

(a) (b) (c)

Fig. 1 – Experimental setup (a) Servo-hydraulic cylinder, (b) setup for 2 x 1 configuration, and (c) setup for 2 x 2 configuration

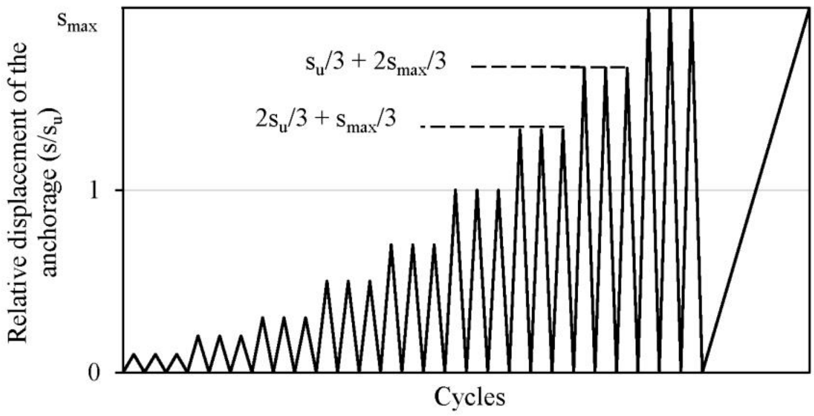

Fig. 2 – Schematic structure of the test procedure for displacement-controlled pulsating tension load

3. Experimental results and discussion

In this section the experimental results are presented. In Fig.3 typical load-displacement curves obtained from the single anchor reference tests and from the tested anchor groups for static and cyclic loading are shown. In Table 2 the experimental results are summarized. The mean ultimate load, the mean displacement at ultimate load and the mean secant stiffness are given for all test series. Concrete cone failure was the observed failure mode in all tests. Typical failure modes are shown in Fig.4.

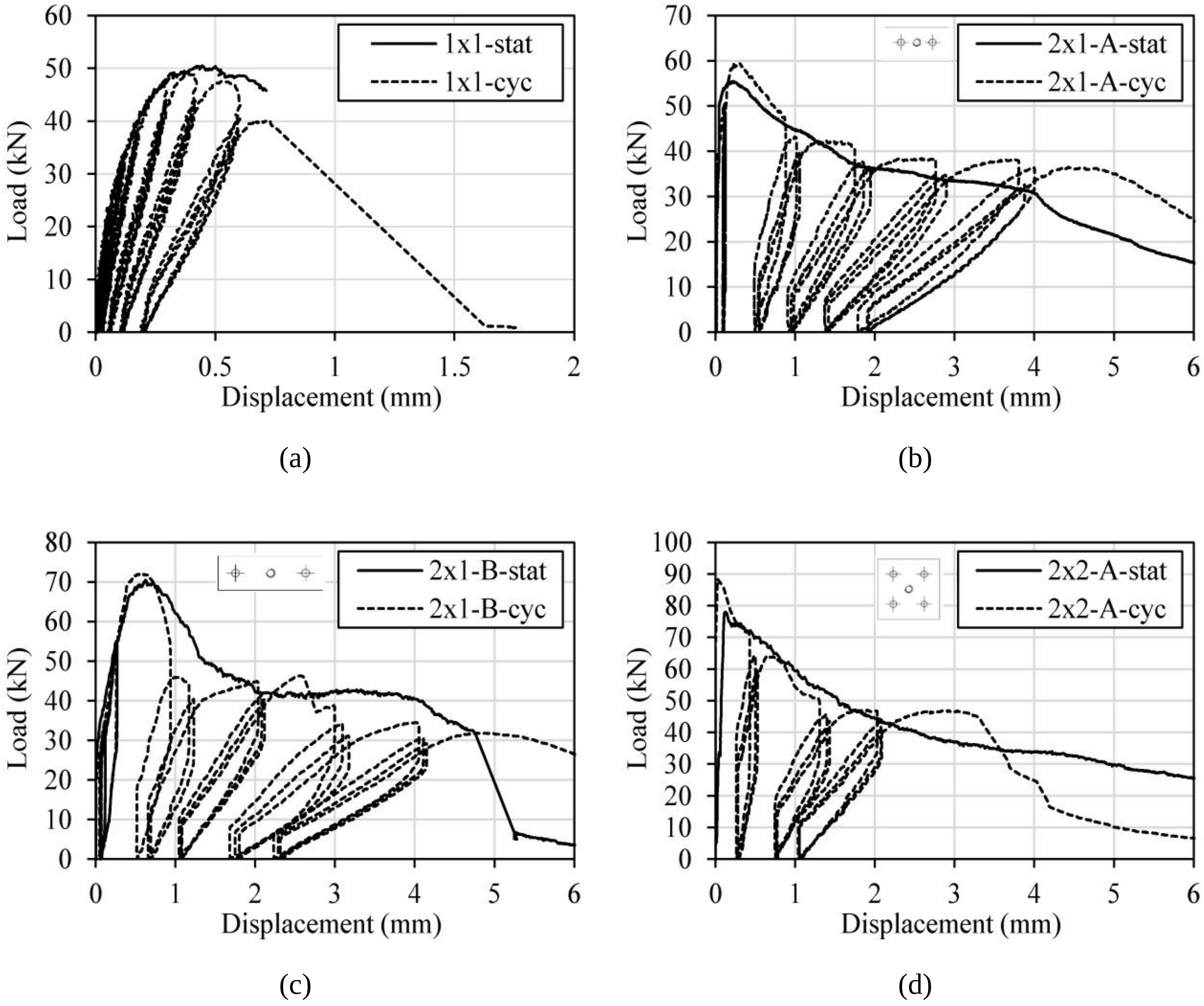

Fig. 3 – Typical load-displacement curves obtained from the tests on single anchors and anchor groups under static and cyclic loading (a) Single anchor, (b) 2x1-A configuration, (c) 2x1-B configuration, and (d) 2x2-A configuration

(a) (b) (c)

Fig. 4 – Typical failure modes (a) 2x1-A configuration, (b) 2x1-B configuration, and (c) 2x2-A configuration

Table 2 – Summary of the experimental results

Test No.	Mean ultimate load, $N_{u,m}$ (kN)	Mean displacement at ultimate load, $s_{u,m}$ (mm)	Mean secant stiffness at ultimate load, $k_{Nu,m}$ (kN/mm)
BA-1x1-stat	49.31	0.556	94.34
BA-1x1-cyc	53.01	0.644	91.58
BA-2x1-A-stat	61.02	0.365	181.38
BA-2x1-A-cyc	60.02	0.289	228.31
BA-2x1-B-stat	68.18	0.635	109.68
BA-2x1-B-cyc	71.16	0.554	129.86
BA-2x2-A-stat	75.48	0.096	802.56
BA-2x2-A-cyc	82.10	0.117	837.12

As can be seen from the load-displacement curves, the envelopes of the cyclic curves in all tests approximately follow the corresponding static curves. Also, the mean ultimate loads of the cyclic tests are in a good agreement with the ultimate loads obtained from the static tests. The only exception are the tests on the quadruple anchor group, where a significant increase in the mean ultimate load was observed in the cyclic tests. The reason for this is that in the static tests, one test deviated widely from the other two tests with a relatively low ultimate load and in the cyclic tests, one test varied from the other tests with a higher ultimate load. Nevertheless, the test results support the conclusion, that cycling has no negative influence on the overall load-displacement behavior of an anchor group, which was also shown in [12]. This also applies for the behavior in the post-peak range of the load-displacement curve. Due to the displacement-controlled protocol, a strength degradation in subsequent cycles was observed, which is particularly true in the post-peak range. Furthermore, significant residual displacements were observed when the anchor groups were unloaded in the post-peak range. This can have a negative effect on structural connections and can significantly influence the performance of a strengthening solution. Comparing the behavior of multiple-anchor groups to the behavior of the reference single anchors, it can be seen that in case of the BA-2x1-A configuration the ultimate load increased by around 19%, in case of the BA-2x1-B configuration the ultimate load increased by around 36% and in case of the quadruple anchor group (2 x 2) the ultimate load increased by around 54%. In case of the 2 x 1 configurations it was observed, that due to the larger spacing of the BA-2x1-B configuration the overall stiffness of the anchor group was significantly lower than for the BA-2x1-A configuration. It appears that for the 160 mm spacing the baseplate cannot be considered as stiff enough and hence the baseplate has a significant influence on the displacement behavior of the group, resulting in a less stiff behavior. In case of the quadruple anchor group the stiffness significantly increased compared to the single anchors and is also significantly higher compared to the 2 x 1 configurations.

4. Numerical study

4.1 Finite element code MASA

The 3D finite element software MASA (Macroscopic Space Analysis), which was developed at the Institute of Construction Materials, University of Stuttgart for the non-linear analysis of concrete and RC structures, was used to perform the numerical simulations in this work. The constitutive law for concrete is based on the microplane model with relaxed kinematic constraint proposed by [13] and a smeared crack approach is applied to realistically simulate the damage and fracture phenomena. Planes of various orientation which can be interpreted as damage planes on a microstructural level, e.g. the contact layer between aggregates in case of concrete, form the basis of the microplane model. In case of softening (quasi brittle) materials, such as concrete, the uniqueness of the solution can be guaranteed by replacing the static constraint by kinematic constraint. Therefore, the strain components on the microplanes are calculated as the projection of the macroscopic strain tensor. In case of tensile loading, the decomposition of the normal strain component can lead to a pathological behavior. This is why the microplane strain components are modified in order to relax the kinematic constraint. A problem in the finite element analysis is, that the results can vary significantly depending on the element size. This effect can be evaded by implementing so-called localization limiter in the model, which ensure the independence of the total energy consumption from the element size. The finite element software MASA uses the crack band method to guarantee mesh independence [14]. To model the steel elements, such as the anchor rods and the baseplate, a linear-elastic material behavior is assumed. This assumption is made on the basis, that concrete failure is expected for the given problem, before yielding of the steel in the anchors or in the baseplate. In this way the computational time can be reduced.

4.2 Numerical models

Three unreinforced concrete slabs were modelled for the numerical simulations. The first slab, where the anchor group is placed far away from all the edges, was modelled with a side length of 1200 mm and a thickness of 300 mm. This model is used to validate the numerical modeling approach against the experimental results. The second slab was modelled with a length of 1200 mm, a width of 250 mm (narrow member) and a thickness of 300 mm. In this slab the anchor group is placed close to two parallel edges, with an edge distance of c_1 = 85 mm on each side, such as to simulate anchorage in a beam type concrete member. In the third slab, the anchor group is placed close to three edges, with two parallel edges as in the second model and a third edge perpendicular to the other two edges, with an edge distance c_2 = 80 mm. This was done to simulate the situation where the anchorage is used at the end of a beam-type structural member. The length of the third slab is 720 mm, the width is 250 mm and the thickness is 300 mm. The multiple-anchor groups consist of four bonded anchors and the baseplate and represents the quadruple configuration which was tested in the experiments. Hence, the baseplate is modelled with a side length of 160 mm and a thickness of 25 mm. The diameter of the anchors is d_s = 16 mm and they are embedded in the concrete with an effective embedment depth of h_{ef} = 80 mm. The anchor spacing in each direction is $s_1 = s_2$ = 80 mm. The concrete is modelled using 4-node tetrahedral elements and 8-node hexahedral elements are used to model the anchor rods and the baseplate. To model the bond between steel and concrete 2-node bar elements are used which are able to transfer compression and shear forces. The contact between the baseplate and concrete is modeled using compression only 2-node contact elements. The discretization of three concrete slabs, the anchor rods and the baseplate are shown in Fig.5. The material properties for concrete are defined to match the concrete properties used in the experiments. The Young's modulus is E_c = 30420 N/mm², the Poisson's ratio is ν_c = 0.18, the concrete tensile strength is f_t = 2.32 N/mm², the concrete cylinder compressive strength is f_c = 21.45 N/mm² and the fracture energy is G_f = 0.07 N/mm. For steel, only Young's modulus (E_s = 200000 N/mm²) and Poisson's ratio (ν_s = 0.33) had to be defined, since steel is considered as linear elastic. The load is directly applied to the nodes in terms of displacement and is stepwise increased in displacement increments of 0.02 mm. In case of centric loading the load is applied in the middle of the baseplate and in case of eccentric loading the load is applied with an eccentricity of 40 mm in the x-direction. The total force is calculated from the sum of forces in the direction of the applied displacement on the loaded nodes. Likewise, the constraints are directly applied to the nodes. To represent the support conditions of the experiments as shown in Fig.1, two curves on the upper side of the concrete slab are modelled and constraints are applied onto them in the loading direction. To allow the formation of a full concrete cone breakout body, the curves are located 160 mm (= 2*h_{ef}) away from the outermost anchors. The bottom nodes of the concrete slab are constraint perpendicular to the loading direction (in this case in the x- and y-direction) to prevent sliding.

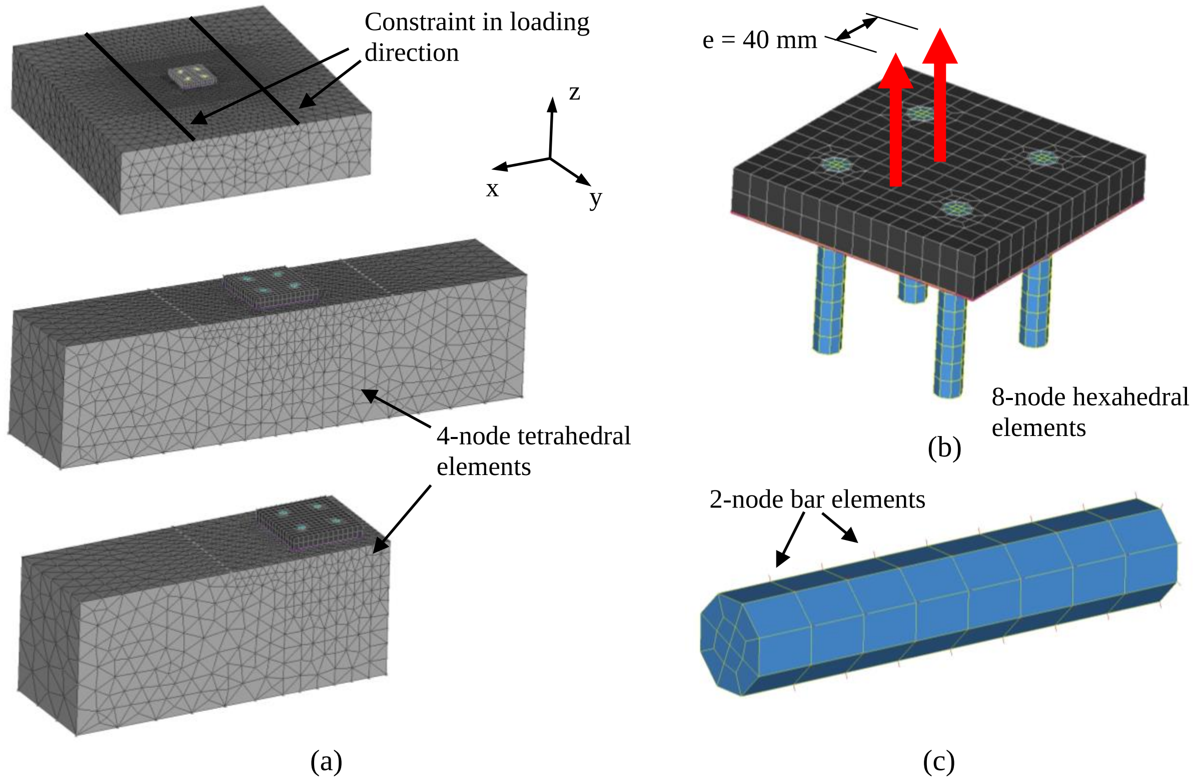

Fig. 5 – FE Models (a) Complete models, (b) Discretization of fixture and anchor rods, and (c) Anchor rod with 2-node bar elements for bond

4.3 Numerical results

In this section the results obtained from the numerical parameter study are discussed. The following two parameters have been considered (i) influence of close edges and (ii) influence of eccentric loading. Furthermore, the numerical model is validated against the experimental results. Fig.6(a) shows the load-displacement curve obtained from the numerical simulation and the load-displacement curve of the statically loaded quadruple anchor group obtained from the experiments. Comparing the experimental results with the results from the simulation of the centrically loaded anchor group away from the edge (Num-2x2-A-stat), it can be seen that the ultimate loads are essentially identical. Also, the stiffness in the ascending branch of the load-displacement curves match well. However, the secant stiffness at ultimate load obtained from the simulation is lower than in the experiments. The main difference between the experiments and the simulation is the behavior in the post-peak range. As can be seen, in the simulation the failure is more brittle than in the experiments and hence the load-displacement curve in the descending branch is steeper than in the experiments. In Fig.6(b) the experimentally and numerically obtained crack patterns are shown. The crack pattern in the numerical model is depicted in terms of the principal tensile strain and red elements represent crack width larger than 0.1 mm. Comparing the crack pattern, it can be seen that the numerically obtained failure mode is in a good agreement with the experimental findings. Therefore, it can be concluded that the numerical simulations reflect the real anchor behavior with a sufficient degree of accuracy.

The numerical results, presented in Fig.7, show that placing the anchor group close to two or three edges appears to have no significant influence on the load-bearing capacity of the anchorage. The ultimate load decreases around 6% and 8% for two and three close edges respectively. Turning to the stiffness a slight stiffness increase at ultimate load was observed with an in increase by around 10% and 12% for two and three close edges respectively. The major difference can be observed in the post-peak range. When the anchor groups are placed close to the edge, the descending branch of the curve shows a more severe drop than for the cases when the anchor group is placed away from the edge.

On the other hand, the results clearly show the negative influence of eccentric loading. Compared to centric loading the ultimate load in all simulations decreased by around 18% – 24%. This is due to the uneven loading of the anchors within the group and the prying action of baseplate. Also, a slight reduction in the stiffness is noticed in all cases with eccentricity, as can be seen in Fig.7. For the case when the anchor group is placed close to three edges, two different eccentricities were considered. In the first case, the eccentric load was placed away from the edge (Num-three_edges-ecc-1) and in in the second case the eccentric load was placed close to the edge (Num-three_edges-ecc-2). When the load was applied close to the edge, the ultimate load was slightly lower than when placed away from the edge.

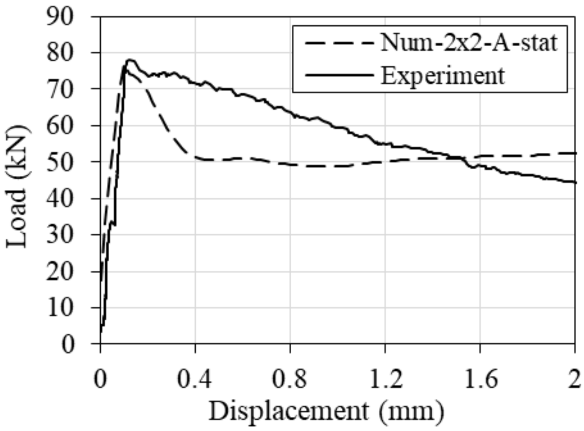

(a)

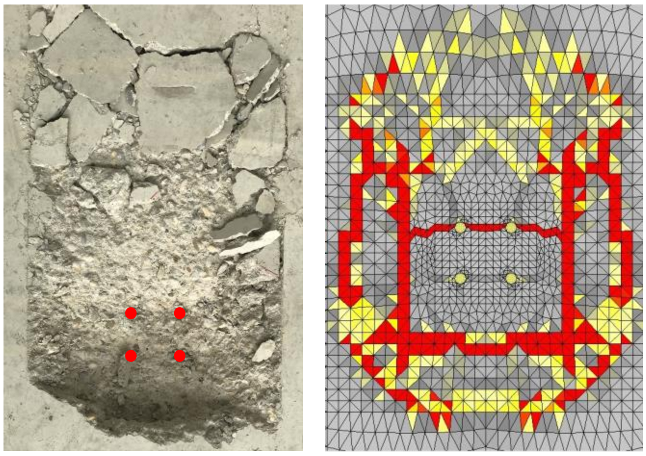

(b)

Fig. 6 – Comparison of experimental and numerical results for the 2 x 2 configuration (a) load-displacement curves (b) obtained crack pattern

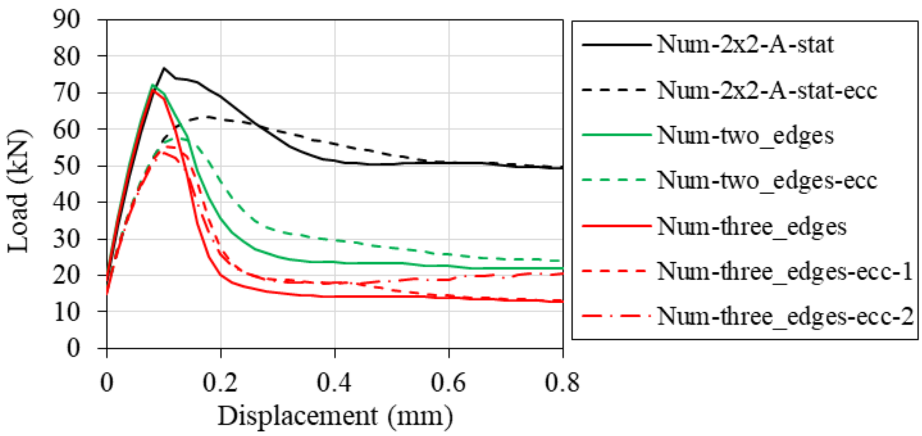

Fig. 7 – Numerical results

5. Conclusion

The focus of the present work was to establish the basis for a better understanding of the displacement behavior and the hysteretic behavior of anchor groups under static and cyclic tension load. Therefore, experimental tests have been performed on various anchor groups and the influence of close edges and eccentric loading was investigated in a numerical parameter study. In the experiments, three different anchor configurations were tested under static and cyclic loading, using a displacement-controlled protocol for pulsating tension load which allows to assess the cyclic and hysteretic behavior of the anchor group in the post-peak range of the load-displacement curve. In the numerical parameter study, seven models have been simulated in order to investigate the influence of two and three close edges. Furthermore, the anchor groups were exposed to eccentric loading while placed close to the edges. From the experimental and numerical results, the following conclusions can be drawn:

1. The experimental results have shown that the envelope of the cyclic load-displacement curves essentially follow the corresponding static curves. Cycling at ultimate load and beyond ultimate load appears to have no negative influence on the overall behavior of the anchor group.
2. Upon unloading of the anchor groups in the post-peak range of the load-displacement curve, residual displacements at zero load were observed. Furthermore, when reloaded to the same displacement level, the anchor groups were not able to take up the same load as in the first cycle of the displacement level. When used in structural strengthening applications these effects can have a significant influence on the success of the strengthening solution and it becomes obvious that these effects should be accounted for in the design process.
3. The baseplate stiffness has a major influence on the displacement behavior of an anchor group. This was shown when the spacing between the anchors in the 2 x 1 configuration was doubled and as a result the stiffness of the complete group decreased significantly.
4. A comparison with the experimental results has shown that the numerical simulation, using the 3D finite element software MASA, can accurately calculate the load-displacement behavior of anchor groups installed in concrete.
5. The results of the numerical parameter study indicate that the edge distance of approximately h_{ef}, had no significant influence on the load-bearing capacity of the anchor group. However, the anchor group failed in a more brittle manner when placed close to the edge.
6. Eccentric loading had a more pronounced negative influence on the load-bearing capacity of the anchor group, with a decrease of the ultimate load by 18% – 24% compared to centric loading. Varying the point of action of the eccentric load from close to the edge to further away from the edge had only a minor effect on the overall load-bearing capacity. This might be attributed to the fact that the investigated quadruple anchor group had relatively small anchor spacing and was relatively stiff. Experimental results, reported in [15], have shown that the point of action (close to the edge and away from the edge) can have a significant influence. Further studies with larger spacing and different configurations are required to investigate the effect more closely.

6. Acknowledgements

The researches wish to thank fischerwerke GmbH & Co. KG for their financial support and the provided equipment. Opinions, conclusions and recommendations expressed in this paper are those of the authors and do not necessarily reflect those of the sponsoring organization.

7. References

[1] Kam WY, Pampanin S, Elwood K (2011): Seismic Performance of Rein-forced Concrete Buildings in the 22 February Christchurch (Lyttelton) Earthquake. *Bulletin of the New Zealand Society for Earthquake Engineering*, **44** (4), 239-78.

[2] Ricci P, De Luca F, Verderame GM (2011): 6th April 2009 L’Aquila earthquake, Italy: reinforced concrete building performance. *Bulletin of Earthquake Engineering*, **9** (1), 203-211.

[3] Watanabe F (1997): Behavior of Reinforced Concrete Buildings during the Hyougoken-Nanbu Earthquake. *Cement and Concrete Composites*, **19** (3), 492-502.

[4] Liel AB, Haselton CB, Deierlein GG (2011): Seismic Collapse Safety of Reinforced Concrete Buildings. II: Comparative Assessment of Nonductile and Ductile Moment Frames. *Journal of Structural Engineering*, **137** (4), 492-502.

[5] Sadjadi R, Kianoush MR, Talebi S (2007): Seismic performance of reinforced concrete moment resisting frames. *Engineering Structures*, **29** (9), 2365-2380.

[6] Mahrenholtz C, Lin PC, Wu AC, Tsai KC, Hwang SJ, Lin RY, Bhayusukma MY (2015): Retrofit of reinforced concrete frames with buckling-restrained braces. *Earthquake Engineering & Structural Dynamics*, **44** (1): 59-78.

[7] Sharma A (2013): Seismic Behavior and Retrofitting of RC Frame Structures with Emphasis on Beam-Column Joints – Experiments and Numerical Modeling. *Ph.D. Thesis*, University of Stuttgart, Germany.

[8] Sharma A (2019): Urgent need for a performance-based approach for seismic assessment and design of fastenings used in structural applications. *Advancements in Civil Engineering & Technology*, **3** (1).

[9] ETA-17/0979 (2018): European Technical Assessment ETA-17/0979 for fischer injection system FIS EM Plus. Deutsches Institut für Bautechnik, Berlin.

[10] Stehle EJ, Sharma A (2020): A new displacement-based approach for pulsating tension load tests of post-installed anchors for the use in structural applications under seismic actions. To be published in *Engineering Structures*.

[11] Stehle EJ, Sharma A (2019): A new assessment approach for post-installed anchors used in seismic applications. *7th International Conference of Euro Asia Civil Engineering Forum (EACEF)*, Stuttgart, Germany.

[12] Eligehausen R, Mallee R, Silva JF (2006): *Anchorage in Concrete Construction*. Berlin: Ernst & Sohn, Germany.

[13] Ožbolt J, Li Y, Kožar I (2001): Microplane model for concrete with relaxed kinematic constraint. *International Journal of Solids and Structures*, **38** (16), 2683-2711.

[14] Ožbolt J: MASA: Finite element program for 3D nonlinear analysis of concrete and reinforced concrete structures. *Manual*, Institute of Construction Materials, University of Stuttgart, Germany.

[15] Bokor B, Sharma A, Hofmann J (2019): Experimental investigations on concrete cone failure of rectangular and non-rectangular anchor groups. *Engineering Structures*, **188**, 202-217.

